

## Observation of a Nuclear-Magnon Contribution to the Nuclear Spin-Lattice Relaxation of $^{191}\text{Pt}$ in Ferromagnetic Cobalt

G. Seewald, E. Hagn, and E. Zech

*Physik-Department, Technische Universität München, D-85748 Garching, Germany*

(Received 27 February 1997)

We report the first indication for a nuclear spin-lattice relaxation mechanism originating from the coupling of the impurity nuclei to nuclear magnons. The magnetic hyperfine interaction and the nuclear spin-lattice relaxation of  $^{191}\text{Pt}$  ( $T_{1/2} = 2.8$  d) in fcc Co were measured with NMR on oriented nuclei at temperatures between 8 and 14 mK in external magnetic fields  $B_{\text{ext}} = 0.1\text{--}10$  kG. Between  $B_{\text{ext}} = 5$  and 1 kG the relaxation rate increases by 2 orders of magnitude. This increase is attributed to the interaction of  $^{191}\text{Pt}$  with nuclear magnons originating from the  $^{59}\text{Co}$  nuclear spin system. [S0031-9007(97)03473-X]

PACS numbers: 76.60.Es, 75.30.Ds, 75.50.Cc, 76.80.+y

The nuclear spin-lattice relaxation (NSLR) of impurity nuclei in the ferromagnetic host lattices Fe, Co, and Ni has been the subject of many investigations, both experimental and theoretical [1–11]. Nevertheless, not all mechanisms which are responsible for the relaxation process are understood in detail.

The strength of the NSLR is described by a relaxation rate,

$$R = 1/C_K, \quad (1)$$

where  $C_K$  is a specific constant for each impurity-host system, analogous to the Korringa constant. At present, it is an open question whether an electronic spin-wave mechanism yields an appreciable contribution to the relaxation rate. Weger [1] studied the relaxation in Fe, Co, and Ni. He proposed that there is a strong contribution to the relaxation rate which originates from the interaction of the conduction electrons with the nuclei via electronic spin waves. Moriya [2] performed calculations including  $d$ -band electrons in a tight-binding approximation. He found that the predominant NSLR mechanism comes from the fluctuation of the orbital current of the  $d$ -band electrons and that the electronic spin-wave contribution is smaller by 1 or 2 orders of magnitude. *Ab initio* calculations of the NSLR rates were started by Kanamori *et al.* [3]. In 1988, Akai [4] published such calculations for all elements as impurities in Fe (with the exception of the rare earths and actinides), in which electronic spin-wave processes were not included. A comparison of the calculated rates with experimental rates shows a unique trend. All calculated rates are too small by a factor of 2–5. This can be interpreted as an indication that an important relaxation mechanism is missing in his model [5]. At present, however, it cannot be stated whether this missing mechanism is the relaxation via electronic spin waves.

As another experimental fact, it was early found that the relaxation rate depends on the external magnetic field  $B_{\text{ext}}$  [6–11]: For high fields ( $B_{\text{ext}} \geq 6$  kG), the relaxation rate is field independent ( $R_\infty$ ); for small fields ( $B_{\text{ext}} \leq 1$  kG), the relaxation rate increases by a factor  $\sim 3\text{--}10$ . This

field dependence of the NSLR is still a controversial subject. With NMR, Kontani *et al.* [6] observed an increase of the NSLR rate between high field and zero field for several  $3d$  and  $4d$  impurities in Fe. They tried to explain this field dependence as a relaxation mechanism due to electronic spin waves. The functional dependence of  $C_K$  on  $B_{\text{ext}}$  calculated within their model was, however, very different from the experimental observation [6,7]. A further approach was a phenomenological model, the so-called enhancement factor model [8,9]. For not too small external magnetic fields, this model described moderately well the functional dependence of  $C_K$  on  $B_{\text{ext}}$  for several systems. Based on the measurement of the NSLR with Fe single-crystal samples, Rüter *et al.* [10] and Van Rijswijk *et al.* [11] favored an electronic spin-wave mechanism as the origin. Again, the correct functional dependence of  $C_K$  on  $B_{\text{ext}}$  could not be predicted. Nevertheless, Niesen [12] speculated recently that an electronic spin-wave relaxation mechanism could imply the functional dependence of  $C_K$  on  $B_{\text{ext}}$  as experimentally observed.

Thus, an entirely new approach to the problem seemed to be necessary. The new idea was as follows: With Co as the host lattice, the question can be addressed whether *nuclear* spin waves have an influence on the relaxation behavior of impurity nuclei and whether nuclear spin waves influence the enhancement factor  $\eta$ . The nuclear spin waves are due to a collective coupling of the  $^{59}\text{Co}$  nuclear spins via the long-range Suhl-Nakamura interaction [13,14]. The nuclear-magnon dispersion relation can be influenced experimentally via the external magnetic field *and* the temperature.

In the absence of collective effects, the single-spin-flip resonance frequency  $\nu_0$  of  $^{59}\text{Co}$  in Co is given by

$$\nu_0 = |g\mu_N(B_{\text{HF}} + B_{\text{ext}})/h|, \quad (2)$$

where  $g$  is the nuclear  $g$  factor and  $B_{\text{HF}}$  is the magnetic hyperfine field. The frequency  $\nu_{k=0}$  of the  $k = 0$  nuclear-magnon excitation mode is given by the relation [15,16],

$$\nu_{k=0}^2 = \nu_0^2 \left(1 - \eta_x \frac{m_0 \langle I_z \rangle}{M_0 I}\right) \left(1 - \eta_y \frac{m_0 \langle I_z \rangle}{M_0 I}\right). \quad (3)$$

Here  $\eta_x$  and  $\eta_y$  are the enhancement factors in the  $x$  and  $y$  direction, respectively, i.e., perpendicular to the orientation axis ( $\eta$  takes into account the enhancement of an external magnetic field at the nuclear site by the hyperfine interaction),  $m_0$  is the saturation value of the nuclear magnetization,  $M_0$  is the saturation value of the electronic magnetization, and  $\langle I_z \rangle / I$  is the fraction of nuclear polarization of the  $^{59}\text{Co}$  spin system. In first order, the frequency shift  $\delta\nu_p = \nu_{k=0} - \nu_0$  is given by

$$\delta\nu_p = -\nu_0 \frac{\eta_x + \eta_y}{2} \frac{m_0 \langle I_z \rangle}{M_0 I}. \quad (4)$$

The nuclear-magnon frequencies lie between  $\nu_0$  ( $k = \infty$ ) and  $\nu_{k=0}$  ( $k = 0$ ). The upper bound  $\nu_0$  is fixed; the lower bound  $\nu_{k=0}$  depends on the external magnetic field (via  $\eta_{x,y}$ ) and on the temperature (via  $\langle I_z \rangle / I$ ). Thus, by the proper choice of  $B_{\text{ext}}$  and/or  $T$ , the nuclear-magnon spectrum may be adjusted to overlap with the resonance frequency of the impurity nuclei. In this context the system  $^{191}\text{PtCo}^{\text{(fcc)}}$  was viewed to be the most promising. The zero-field single-spin-flip resonance of  $^{59}\text{CoCo}^{\text{(fcc)}}$  is deduced as follows: With the hyperfine splitting of  $^{60}\text{CoCo}^{\text{(fcc)}}$  of 125.08(1) MHz and the known ratio of  $g$  factors,  $g(^{60}\text{Co})/g(^{59}\text{Co}) = 0.5747(2)$  [17],  $\nu(^{59}\text{CoCo}^{\text{(fcc)}}) = 217.6(1)$  MHz is obtained.

Samples of  $^{191}\text{PtCo}^{\text{(fcc)}}$  were prepared in the following way: Commercially available Co foils (thickness 2  $\mu\text{m}$ ) were electrically heated for  $\sim 3$  m to  $\sim 1000^\circ\text{C}$  and then quenched to room temperature within  $\leq 1$  s. In this way the hcp structure of Co (this is the stable structure for  $T < 420^\circ\text{C}$ ) is strongly suppressed. The radioactive  $^{191}\text{Pt}$  nuclei were recoil-implanted into Co using the nuclear reaction  $^{192}\text{Os}(\alpha, 5n)^{191}\text{Pt}$ . The  $^{191}\text{PtCo}^{\text{(fcc)}}$  samples were soldered to the cold finger of a  $^3\text{He}$ - $^4\text{He}$ -dilution refrigerator with a top-loading facility, and cooled down to a temperature of  $\sim 10$  mK. An external magnetic field  $B_{\text{ext}} = 0.1$ – $10$  kG was applied to orient the ferromagnetic domains of fcc Co. The  $\gamma$  rays were detected with four Ge detectors placed at  $0^\circ$ ,  $90^\circ$ ,  $180^\circ$ , and  $270^\circ$  with respect to the direction of the external magnetic field. The temperature of the cold finger was measured via the  $\gamma$  anisotropy of a  $^{60}\text{CoCo}^{\text{(hcp)}}$  nuclear thermometer.

First, the nuclear magnetic resonance on oriented nuclei (NMR-ON) signal of  $^{191}\text{PtCo}^{\text{(fcc)}}$  was measured for  $B_{\text{ext}} = 0.1, 1, 2, 3, 5,$  and  $10$  kG. The spectra for  $B_{\text{ext}} = 3$  and  $5$  kG are shown in Fig. 1. Here, successively measured spectra with frequency modulation (FM) (modulation bandwidth  $\Delta f_{\text{mod}} = \pm 0.3$  MHz) and without FM ( $\Delta f_{\text{mod}} = 0$ ) were subtracted. In all FM-off spectra the resonance amplitude was zero. The resonance centers are shown as circles in Fig. 2. From a *least-squares fit* (solid line in Fig. 2) we obtain  $\nu(B_{\text{ext}} = 0) = 203.14(7)$  MHz and  $d\nu/dB_{\text{ext}} = -0.257(10)$  MHz/kG. The shift of the resonance with  $B_{\text{ext}}$  is in good agreement with the expectation taking into account the known  $g$  factor of  $^{191}\text{Pt}$ :  $d\nu/dB_{\text{ext}} = -0.255(2)$  MHz/kG. The half-width  $\Gamma$  of

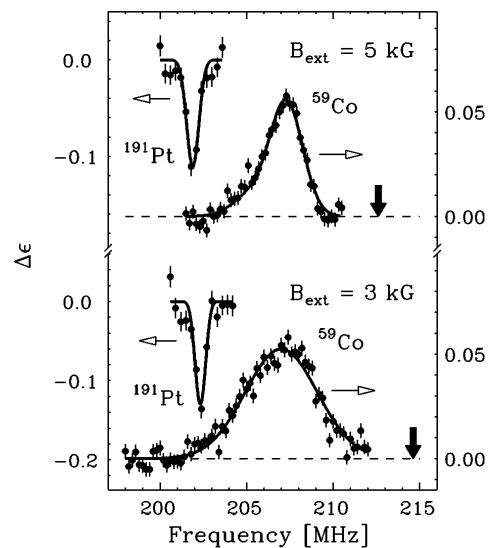


FIG. 1. NMR-ON resonances of  $^{191}\text{PtCo}^{\text{(fcc)}}$  (sharp resonances) and calorimetrically detected rf absorption by  $k = 0$  nuclear magnons (originating from the collective coupling of  $^{59}\text{Co}$  nuclear spins) measured for  $B_{\text{ext}} = 5$  (top) and  $3$  kG (bottom) at a temperature of  $14(1)$  mK. The single-spin-flip hyperfine interaction of  $^{59}\text{CoCo}^{\text{(fcc)}}$  is marked with bold arrows. With decreasing  $B_{\text{ext}}$ , the frequency difference between the  $k = 0$  nuclear-magnon excitation mode and the single-spin-flip hyperfine interaction of  $^{59}\text{CoCo}^{\text{(fcc)}}$  becomes larger. Additionally, the frequency width of the  $k = 0$  nuclear-magnon mode increases. Thus, an overlap of the  $^{191}\text{PtCo}^{\text{(fcc)}}$  resonance with the  $k = 0$  nuclear-magnon mode occurs for  $B_{\text{ext}} < 3$  kG.  $\Delta\epsilon$  is the resonant change of the  $\gamma$  anisotropy  $\epsilon = W(0^\circ)/W(90^\circ)$ , where  $W(\vartheta)$  is the angular distribution of  $\gamma$  rays emitted in the decay of oriented nuclei.

the NMR-ON resonances showed no dependence on  $B_{\text{ext}}$ ; the average value of  $\bar{\Gamma} = 0.75(5)$  MHz indicates a high quality of the fcc structure of the Co foils. At the known frequency for  $^{191}\text{Pt}$  in hcp Co [18], no resonance signal was observed.

Second, the resonance of the  $^{59}\text{CoCo}^{\text{(fcc)}}$  system was measured for  $T = 14(1)$  mK by calorimetric NMR. Here the rf was applied unmodulated. The resonance absorption of the radio frequency causes a temperature increase of the sample (and hence of the sample holder and the  $^{60}\text{CoCo}^{\text{(hcp)}}$  thermometer) which was observed via the  $\gamma$  anisotropy of the  $^{60}\text{CoCo}^{\text{(hcp)}}$  thermometer. The spectra for  $B_{\text{ext}} = 3$  and  $5$  kG are shown in Fig. 1. The maxima of the broad resonance structures are located significantly below the  $^{59}\text{CoCo}^{\text{(fcc)}}$  single-spin-flip resonance (marked with bold arrows). The resonance centers are shown in Fig. 2. They coincide well with the expectation calculated according to Eq. (3) for  $T = 14$  mK (dotted line). From the fact that the resonance structure could be excited with unmodulated rf, we must conclude that the width of the resonance is due mainly to homogeneous broadening. (The large homogeneous linewidth is due to a short spin-spin relaxation time originating from the strong coupling

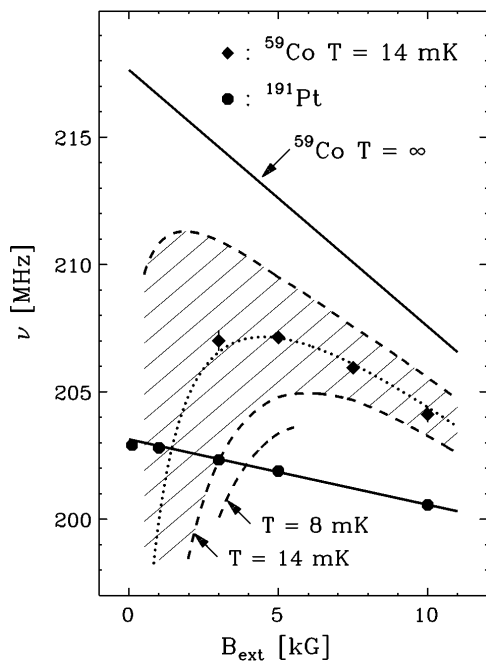


FIG. 2. Resonance centers of the NMR-ON resonances of  $^{191}\text{PtCo}^{(\text{fcc})}$  (circles) and  $^{59}\text{CoCo}^{(\text{fcc})}$  (diamonds) for  $T = 14(1)$  mK. The dotted line represents the theoretical resonance frequency for the  $^{59}\text{Co}$   $k = 0$  nuclear-magnon excitation mode according to Eq. (3). The agreement with the measured values is remarkably good. The shaded area enveloped by the dashed curves represents the  $2\sigma$  frequency region in which 95% of the rf absorption by the nuclear-magnon excitations takes place. In addition, the calculated lower bound for the 95%-absorption region for  $T = 8(1)$  mK is shown by a dashed curve. It is evident that the overlap region between the  $^{191}\text{PtCo}^{(\text{fcc})}$  resonance and the  $k = 0$  nuclear-magnon excitation mode shifts to a higher value of  $B_{\text{ext}}$  with decreasing temperature.

of the  $^{59}\text{Co}$  nuclear spins.) Thus we conclude that the observed resonance structure represents the  $k = 0$  nuclear-magnon excitation mode. Attempts to measure the resonance for  $B_{\text{ext}} = 1$  kG failed, most probably because of the fact that the linewidth at low magnetic fields becomes so large that the statistical accuracy obtainable within reasonable measurement times was not sufficient to resolve the resonance. There is no theoretical prediction on the width of this resonance. Experimentally, it was found that the width increases with decreasing external magnetic field: For  $B_{\text{ext}} = 10, 7.5, 5,$  and  $3$  kG, the half-width was found to be  $\Gamma = 1.45(15), 1.75(10), 2.7(2),$  and  $4.9(3)$  MHz, respectively. The shaded area in Fig. 2 represents the frequency region in which 95% of the absorption by the  $k = 0$  nuclear magnons takes place. The frequency difference between the  $^{191}\text{PtCo}$  and the  $^{59}\text{CoCo}$  resonance depends strongly on the external magnetic field: Below  $3$  kG, the overlap between the  $^{191}\text{Pt}$  resonance and the  $k = 0$  nuclear-magnon excitation mode becomes strong. Lowering the temperature, this overlap region can be shifted to higher values of  $B_{\text{ext}}$ . This is due to the dependence

of  $\nu_{k=0}$  on  $\langle I_z \rangle / I$  [see Eq. (4)]. To illustrate this, the calculated lower bound of the 95% absorption region for  $T = 8$  mK is also shown in Fig. 2. Thus, the overlap of the  $^{191}\text{PtCo}^{(\text{fcc})}$  resonance with the  $k = 0$  nuclear-magnon excitation mode can be forced by a proper choice of the external magnetic field and the temperature.

Third, we measured the spin-lattice relaxation of  $^{191}\text{PtCo}^{(\text{fcc})}$  as a function of  $B_{\text{ext}}$  with the commonly used technique of switching the frequency modulation. The first measurements were performed for  $T = 8(1)$  mK. The relaxation spectra for  $0.1$  and  $10$  kG are shown in Fig. 3. Note that the time scales differ by 2 orders of magnitude. The solid lines are the result of least-squares fits. The theoretical curves are multiexponential functions which are obtained by solving the rate equations with the Korringa constant  $C_K$  and the rf coupling  $C_{\text{HF}}^{(\text{app})} \eta^2$  as free parameters. (The rf coupling constant  $C_{\text{HF}}^{(\text{app})}$  is proportional to the power  $P_{\text{app}}$  of the applied rf field.) The relaxation rate  $C_K^{-1}$  as a function of  $B_{\text{ext}}$  is shown in Fig. 4. For  $0 < B_{\text{ext}} < 1$  kG and  $5 < B_{\text{ext}} < 10$  kG, it is nearly constant; from  $B_{\text{ext}} = 5$  to  $1$  kG, it increases by about 2 orders of magnitude. The fast relaxation occurs in the frequency region, for which, as illustrated in Fig. 2, the  $^{191}\text{Pt}$  resonance overlaps with the  $k = 0$

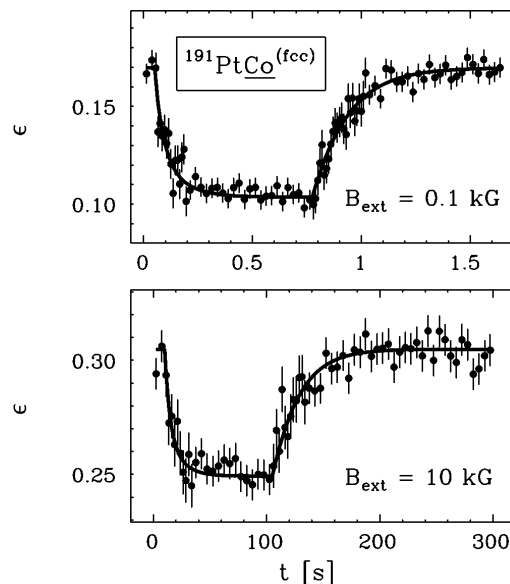


FIG. 3. Nuclear spin-lattice relaxation measurements on  $^{191}\text{PtCo}^{(\text{fcc})}$  for  $B_{\text{ext}} = 0.1$  kG (top) and  $10$  kG (bottom):  $\gamma$  anisotropy  $\epsilon$  vs time. The resonant excitation of the  $^{191}\text{Pt}$  nuclei and the subsequent relaxation to thermal equilibrium were controlled by switching the frequency modulation bandwidth between  $\Delta f_{\text{mod}} = 0$  ("FM off") and  $\Delta f_{\text{mod}} = \pm 1.2$  MHz ("FM on"). (By applying the rf permanently and switching the FM instead of the rf power, it is excluded that time-dependent warming effects by eddy-current heating influence the measurements.) Both measurements were performed with the same rf power. Note that the time scales differ by 2 orders of magnitude.

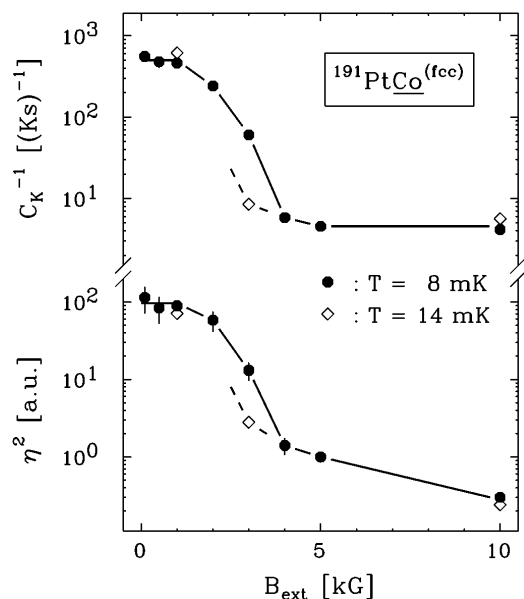


FIG. 4. Top: experimental relaxation rate of  $^{191}\text{PtCo}^{(\text{fcc})}$  vs  $B_{\text{ext}}$  for  $T = 14(1)$  mK (diamonds) and  $8(1)$  mK (circles). The transition from normal to fast relaxation is shifted to a higher external magnetic field for lower temperature. The solid lines indicate the experimental trend. Bottom: experimental enhancement factor for the rf field. Note that the functional dependences of the relaxation rate and the rf enhancement factor on  $B_{\text{ext}}$  are slightly different. The solid lines indicate the experimental trend.

nuclear-magnon excitation mode. As discussed above, this overlap region can be shifted with the temperature. At higher temperatures, the transition from slow to fast relaxation should occur at a smaller external magnetic field. Therefore additional relaxation measurements were performed for  $T = 14(1)$  mK. The results are shown with open symbols in Fig. 4. Whereas there is no difference in the relaxation rates for  $B_{\text{ext}} = 1$  and  $10$  kG, a strong difference is observed for  $B_{\text{ext}} = 3$  kG. Here the relaxation rates for  $T = 14$  and  $8$  mK differ by a factor of  $7.1(1.0)$ . (Both measurements were performed with the same rf power. The temperature was varied by heating the mixing chamber.)

The enhancement factor  $\eta$  for the rf field was also determined. The results for  $\eta^2$  (enhancement of the rf power) are shown in the lower part of Fig. 4. It is obvious that the effective rf power at the site of  $^{191}\text{Pt}$  is strongly enhanced by the coupling of  $^{191}\text{Pt}$  to the  $k = 0$  nuclear-magnon excitation mode. The most striking proof is given by the result for  $B_{\text{ext}} = 3$  kG: Here the enhancement factor varies as a function of the temperature. The ratio of  $\eta^2$  for  $T = 14(1)$  and  $8(1)$  mK is  $4.7(1.5)$ . This ratio is slightly smaller than the corresponding ratio of the relaxation rates, which is  $7.1(1.0)$ . In toto, between  $5$  and  $1$  kG,  $C_K^{-1}$  increases by a factor of  $102(16)$ , whereas  $\eta^2$  increases by a factor of  $89(25)$ .

In summary, we have shown that a nuclear-magnon contribution to the nuclear spin-lattice relaxation exists. It is responsible for the increase of the nuclear spin-lattice relaxation rate of  $^{191}\text{Pt}$  in fcc Co by about 2 orders of magnitude. These processes are also responsible for an increase of the enhancement factor for the rf field by about the same amount. On the basis of these results, we conclude that the “normal” magnetic-field dependence of the spin-lattice relaxation originates from the interaction of the impurity nuclei with electronic spin waves. The magnetic field dependence of the enhancement factor is, thus, also a spin-wave excitation property. In the light of these facts, it becomes evident why the enhancement factor model described moderately well the magnetic-field dependence of the normal NSLR. Our experiments suggest that a new theoretical approach should be initiated to describe the spin-lattice relaxation with a complete inclusion of the spin-wave processes.

We wish to thank E. Smolic for experimental help. This work has been funded by the Deutsche Forschungsgemeinschaft (DFG) under Contract No. Ha 1282/3-3 and, partly, by the Forschungszentrum Karlsruhe.

- [1] M. Weger, Phys. Rev. **128**, 1505 (1962).
- [2] T. Moriya, J. Phys. Soc. Jpn. **19**, 681 (1964).
- [3] J. Kanamori, H. Yoshida, and K. Terkura, Hyperfine Interact. **9**, 363 (1981).
- [4] H. Akai, Hyperfine Interact. **43**, 255 (1988).
- [5] C. Bobeck, R. Dullenbacher, and E. Klein, Hyperfine Interact. **77**, 327 (1993).
- [6] M. Kontani, T. Hioki, and Y. Masuda, J. Phys. Soc. Jpn. **32**, 416 (1972).
- [7] Y. Masuda, T. Hioki, and M. Kontani, Int. J. Magn. **6**, 143 (1974).
- [8] M. Kopp and E. Klein, Hyperfine Interact. **11**, 153 (1981).
- [9] E. Klein, in *Nuclear Magnetic Resonance on Oriented Nuclei*, edited by N.J. Stone and H. Postma, Low-Temperature Nuclear Orientation (North-Holland, Amsterdam, 1986), p. 579.
- [10] H.D. Rüter, W. Haaks, E.W. Duczynski, D. Visser, and L. Niesen, Hyperfine Interact. **9**, 385 (1981).
- [11] W. van Rijswijk, H.S. van der Rande, A.A. Jilderda, and W.J. Huiskamp, Hyperfine Interact. **39**, 23 (1988).
- [12] L. Niesen (private communication).
- [13] H. Suhl, Phys. Rev. **109**, 606 (1958).
- [14] T. Nakamura, Prog. Theor. Phys. **20**, 542 (1958).
- [15] P.G. de Gennes, P. Pincus, F. Hartmann-Boutron, and J.M. Winter, Phys. Rev. **129**, 1105 (1963).
- [16] G. Seewald, E. Hagn, and E. Zech, Phys. Lett. A **220**, 287 (1996).
- [17] L. Niesen and W.J. Huiskamp, Physica (Utrecht) **57**, 1 (1972).
- [18] B. Hinfurter, E. Hagn, E. Zech, R. Eder, and ISOLDE Collaboration, Phys. Rev. Lett. **64**, 2188 (1990).